Available online at www.sciencedirect.com

ScienceDirect

IFAC Papers Online CONFERENCE PAPER ARCHIVE

IFAC PapersOnLine 59-9 (2025) 7–12

A cooperative distributed algorithm for handling reactive power saturation in active distribution networks ⋆

G.M. Casolino * **G. Fusco** * **M. Russo** *

* *Department of Electrical and Information Engineering, University of Cassino and Southern Lazio, Via G. Di Biasio 43, Cassino (FR), 03043, Italy (e-mail: casolino@unicas.it; fusco@unicas.it; russo@unicas.it).*

Abstract: In Active Distribution Networks (ADNs), voltage regulation can be achieved by local controllers acting on the reactive power injected by Distributed Energy Resources (DERs). An optimization algorithm at the secondary control level evaluates the voltage set points for the local controllers at the primary level. However, the continuous variations of the ADN operating conditions may cause saturation of the reactive powers, which causes the integral wind-up phenomenon of the local PI regulators, leading to degraded performance, as well as the inability to achieve the optimal voltage profile. To manage these issues, the present paper proposes a cooperative strategy among DERs implemented by a distributed algorithm in which all DERs cooperate to solve the saturation. The distributed algorithm locally calculates the variation of the set point of each DER controller to pursue two objectives: avoiding the wind-up phenomenon and achieving a new voltage profile closer to the optimal one. The algorithm uses fixed average weights and does not depend on the control techniques used to design the PI regulators. Only voltage errors are exchanged among DERs, and the communication requirements are limited. The results of accurate numerical simulations give evidence of the validity of the proposed cooperative distributed algorithm.

Keywords: Active distribution networks; Anti-windup; Control of renewable energy resources; Cooperative algorithms; Distributed control; Systems with saturation; Voltage regulation.

1. INTRODUCTION

Distributed energy resources (DERs), including distributed generation, electric energy storage systems, active loads, and electric vehicle charging stations, support the correct operation of active distribution networks (ADNs). In particular, DERs interfacing ADN through power electronic inverters contribute to voltage regulation by acting on their reactive power injection, according to IEEE Std 1547™-2018 and EN 50549.

A hierarchical voltage control structure is generally adopted in ADNs, see Fusco et al. (2021), to fully exploit DER support for voltage regulation. Each DER performs the primary control through a local voltage control loop regulating the nodal voltage at the point of common coupling (PCC). The set points are fixed by the secondary control that optimizes the ADN voltage profile according to appropriate objectives settled by the Distribution System Operator (DSO).

The local voltage controller contains an integral action to achieve a null steady-state voltage regulation error at PCC, Fusco et al. (2023). If the reference reactive power output by the controller is greater than the limit value imposed on the reactive power injected by the DER, the well-known phenomenon called integral wind-up occurs. Generally, most of the design techniques of anti-windup compensation schemes have been developed for SISO plants and, in principle, extended to MIMO systems, thus negatively impacting the achieved performance. Hence, different solutions to this problem have been reported in the literature, resulting in anti-windup compensation schemes for MIMO plants as in Edwards and Postlethwaite (1997); Morilla et al. (2009); Mulder et al. (2001). However, MIMO approaches require a complex design to solve the saturation non-linearity problem and to cope with the time delays associated with real-time communication exchanges among all the controllers. For these reasons, distributed control techniques have recently been proposed as an alternative way to handle the presence of saturation limits by Bidram et al. (2014); Errouissi and Al-Durra (2018); Lin (2019); Zhuang et al. (2022).

A first approach of a distributed cooperative algorithm among DERs was proposed in Robbins et al. (2013) with the basic aim of avoiding voltage violations by equally sharing the need for reactive power among DERs. In this paper, a cooperative algorithm involving all DERs in the presence of saturated reactive powers is proposed, assuming that each DER is equipped with a local voltage closed-loop regulation. If a DER saturates, all other DERs

⋆ The research has been financially supported by Project ECS 0000024 “Ecosistema dell’innovazione - Rome Technopole” financed by EU in NextGenerationEU plan through MUR Decree n. 1051 23.06.2022 PNRR Missione 4 Componente 2 Investimento 1.5 - CUP H33C22000420001

10.1016/j.ifacol.2025.08.104

participate to solve the saturation. In practice, each DER controller receives the voltage errors from all the other DERs and locally calculates the voltage variation of its optimal set point using fixed average weights, which account for the nodal voltage sensitivity coefficients of the network. The new set points pursue a double objective. The first is determining a corresponding variation of the reactive powers injected by DERs that solves the saturation problem by restoring a linear control, thus avoiding wind-up of linear controllers. The second is improving the voltage profile of the ADN by reducing its distance from the optimal one. The execution time interval of the proposed algorithm is much larger than the sampling time of both local controllers and communication links, so the associated delays can be safely assumed to be zero, and the communication requirements are quite limited. Eventually, the effectiveness of the proposed cooperative distributed algorithm is validated by numerical simulations of an ADN with six DERs.

2. COOPERATIVE DISTRIBUTED ALGORITHM

2.1 Model of active distribution network

The steady-state operation of an ADN with N DERs is modeled using the DistFlow equations, Baran and Wu (1989) that exploit the radial configuration of the grid. These equations can be approximated by the well-known LinDistFlow equations, which consist of a linearization of the DistFlow equations neglecting active and reactive power losses. From the LinDistFlow equations, the following representation can be derived by partitioning the graph-based matrix obtained according to Zhu and Liu (2016)

$$\Delta \boldsymbol{V} = \boldsymbol{V} - \boldsymbol{V}^0 = \boldsymbol{\Gamma}\ \boldsymbol{Q} \tag{1}$$

where $\boldsymbol{V}$ and $\boldsymbol{Q}$ are $(N\times 1)$ vectors of voltages and reactive power injections at the N nodes where the DERs are connected, respectively, $\boldsymbol{V}^0$ comprises the voltage values when $\boldsymbol{Q} = \boldsymbol{0}$ and $\boldsymbol{\Gamma}$ is a $(N \times N)$ matrix symmetric and positive definite, see Zhu and Liu (2016). The generic element γ_{ij} in the i^{th} row and j^{th} column position of $\boldsymbol{\Gamma}$ represents the sensitivity of the voltage of the i^{th} DER to the reactive power injection of the j^{th} DER. The way in which $\boldsymbol{\Gamma}$ is constructed guarantees that $\gamma_{ii} \geq \gamma_{ij} > 0$ for all i and j.

Each DER has a PI-based control loop that regulates the voltage at its PCC to an assigned set point by varying its reactive power injection. Hence, the PI regulators guarantee that the vector of voltage errors

$$\boldsymbol{\epsilon} \triangleq \boldsymbol{V}^{sp} - \boldsymbol{V} \tag{2}$$

is null at steady-state, being $\boldsymbol{V}^{sp}$ the vector of set points and $\boldsymbol{V}$ the vector of regulated voltages. The secondary control provides the optimal values $\boldsymbol{V}^{sp,opt}$ for $\boldsymbol{V}^{sp}$ solving appropriate optimization problems. Since these problems account for the reactive power limits as constraints, the set points $\boldsymbol{V}^{sp,opt}$ should not lead DER reactive powers to saturation. It means that the value $\boldsymbol{Q}^*$ resulting from the solution of (1) according to

$$\boldsymbol{Q}^* = \boldsymbol{\Gamma}^{-1}\ \left(\boldsymbol{V}^{sp,opt} - \boldsymbol{V}^0\right) \tag{3}$$

is feasible, and each of its elements satisfies the reactive power limit of the related DER.

In practice, since the optimization task is performed at large time intervals, in between two subsequent optimizations, the value of $\boldsymbol{V}^0$ changes due to the variation of the distribution system operating conditions, mainly caused by variations of loads and active power generation. Then, since the vector of the voltage set point

$$\boldsymbol{V}^{sp} = \boldsymbol{V}^{sp,opt} \tag{4}$$

is not changed, the variations of $\boldsymbol{V}^0$ can result in an unfeasible value $\boldsymbol{Q}^*$ from (3) and in the reactive power saturation of one or more DERs. Consequently, one or more steady-state voltage regulation errors are not null, and the overall performance of the PI control loops is degraded because of the wind-up phenomenon.

2.2 Cooperative strategy

Let's assume for the sake of readability but without loss of generality that the j^{th} DER saturates. From (2) it follows that the steady-state value of $\epsilon_j = V_j^{sp} - V_j$ is not null and, since (4), it is equal to

$$\bar{\epsilon}_j = V_j^{sp,opt} - V_j \tag{5}$$

The simplest way to handle the saturation locally is to impose a variation to the set point equal to

$$\Delta V_j^{sp} = -\bar{\epsilon}_j \tag{6}$$

The new set point becomes $V_j^{sp} = V_j^{sp,opt} - \bar{\epsilon}_j$ and, substituting $\bar{\epsilon}_j$ from (5), $V_j^{sp} = V_j$, that is the voltage regulation error ϵ_j becomes null. The advantage of this approach is that it is strictly local and does not require data exchange between the j^{th} DER and all the others. On the contrary, the main disadvantage is that the difference between $V_j^{sp,opt}$ and V_j remains unchanged and equal to $\bar{\epsilon}_j$, see (5). Consequently, the overall voltage profile differs from the optimal one fixed by the secondary control level.

Differently from (6) that introduces a variation only on the voltage set point of the saturated DER, the proposed cooperation strategy introduces a variation of the set points of all the DERs

$$\boldsymbol{V}^{sp} = \boldsymbol{V}^{sp,opt} + \Delta \boldsymbol{V}^{sp} \tag{7}$$

Hence, the unsaturated DERs also participate in solving the saturation. The aim is twice: not only to desaturate the j^{th} DER, but also to reduce the distance of the voltage profile from the optimal one.

The variations $\Delta \boldsymbol{V}^{sp}$ are evaluated by assigning a share of the error $\bar{\epsilon}_j$ to each DER according to a weighted average principle, where the averaging weights account for the different impact of each DER on ϵ_j. According to (1) this impact is quantified by the elements of the $(N \times 1)$ vector $\boldsymbol{\gamma}_j$ representing the transposed j^{th} row of $\boldsymbol{\Gamma}$ or, equivalently, the j^{th} column of $\boldsymbol{\Gamma}^T$. Then, normalizing the elements of $\boldsymbol{\gamma}_j$, the vector of the weights $\boldsymbol{a}_j$ is derived as

$$\boldsymbol{a}_j = \frac{1}{\left|\boldsymbol{\gamma}_j\right|_1}\boldsymbol{\gamma}_j \tag{8}$$

where $\left|\boldsymbol{\gamma}_j\right|_1$ is the 1-norm of $\boldsymbol{\gamma}_j$. The normalization (8) guarantees a unitary sum of the elements of $\boldsymbol{a}_j$, that is $\left|\boldsymbol{a}_j\right|_1 = 1$. Moreover, from the properties of the elements of $\boldsymbol{\gamma}_j$ it is derived that $a_{jj} \geq a_{ji} > 0$ for all i.

Using the elements a_{ji} of $\boldsymbol{a}_j$ as weights, the variations of the set points for all the unsaturated DERs can be derived as

$$\Delta V_i^{sp} = a_{ji}\,\bar{\epsilon}_j \quad \text{for } i \neq j \tag{9}$$

whereas for the j^{th} DER the variation ΔV_j^{sp} is obtained by adding the variation with the j^{th} weight to (6) according to

$$\Delta V_j^{sp} = -\bar{\epsilon}_j + a_{jj}\,\bar{\epsilon}_j = -(1-a_{jj})\,\bar{\epsilon}_j \tag{10}$$

Adopting (9)–(10) rather than (6) reduces the distance of the resulting voltage profile from the optimal one. This distance can be measured by the Euclidean norm $|\Delta \boldsymbol{V}^{sp}|_2$, with $\Delta \boldsymbol{V}^{sp}$ derived from (7). Applying (6) results in

$$|\Delta \boldsymbol{V}^{sp}|_2 = |\bar{\epsilon}_j| \tag{11}$$

being $|\bar{\epsilon}_j|$ the absolute value of $\bar{\epsilon}_j$, whereas applying (9)–(10) yields

$$|\Delta \boldsymbol{V}^{sp}|_2 = \left(\sum_{i\neq j} a_{ji}^2 + (1-a_{jj})^2\right)^{0.5} |\bar{\epsilon}_j| \; < \; |\bar{\epsilon}_j| \tag{12}$$

The inequality in (12) stands because

$$\sum_{i\neq j} a_{ji}^2 + (1-a_{jj})^2 = \sum_i a_{ji}^2 + 1 - 2a_{jj} \leq 1 - a_{jj} < 1$$

being

$$\sum_i a_{ji}^2 \leq a_{jj} \sum_i a_{ji} = a_{jj}$$

thanks to the properties of $\boldsymbol{a}_j$ and its elements.

The cooperative strategy represented by (8)–(10) can easily be extended to the general case in which multiple DERs suffer reactive power saturation.

Normalizing the elements of $\boldsymbol{\Gamma}^T$ by column, the matrix of the weights is derived as

$$\mathbf{A} = \boldsymbol{\Gamma}^T \; diag\Big\{1/\left|\boldsymbol{\gamma}_1\right|_1, 1/\left|\boldsymbol{\gamma}_2\right|_1, \ldots, 1/\left|\boldsymbol{\gamma}_N\right|_1\Big\} \tag{13}$$

where the second term on the right-hand side represents the diagonal matrix whose j^{th} diagonal element is the reciprocal of $\left|\boldsymbol{\gamma}_j\right|_1$. The normalization (13) guarantees that the columns of matrix $\mathbf{A}$ have unitary sum, that is $|\boldsymbol{a}_j|_1 = 1$ for all j. Then, (9)–(10) can be cast in matrix form as below

$$\Delta \boldsymbol{V}^{sp} = -\mathbf{L}\,\bar{\boldsymbol{\epsilon}} \tag{14}$$

where $\bar{\boldsymbol{\epsilon}}$ is the vector of the elements $\bar{\epsilon}_j$ and

$$\mathbf{L} = \mathbf{I} - \mathbf{A} \tag{15}$$

being $\mathbf{I}$ the $N \times N$ identity matrix.

2.3 Distributed iterative algorithm

From (14), an iterative algorithm is derived, in which the k^{th} iteration step is

$$\boldsymbol{V}^{sp}(k) = \boldsymbol{V}^{sp}(k-1) - \mathbf{L}\,\boldsymbol{\epsilon}(k) \tag{16}$$

being $\boldsymbol{\epsilon}(k) = \boldsymbol{V}^{sp}(k-1) - \boldsymbol{V}(k)$ from (2). Standing the property $|\boldsymbol{a}_j|_1 = 1$ for all j, from (15) it is trivial to derive that $|\boldsymbol{l}_j|_1 = 0$ for all j. Then, since the columns of matrix $\mathbf{L}$ have a null sum, an average equilibrium of the iterative algorithm (16) exists.

The cooperative algorithm (16) is implemented with a distributed approach. At each time step, the DER controllers exchange their voltage regulation errors. Then, each j^{th} DER, using the stored and fixed j^{th} row of matrix $\mathbf{L}$, locally evaluates the new value of its set point, according to (16). The time step of the algorithm should be large enough to assume that the transient response of the voltage control loop is extinguished and compatible with the features of the communication channels among the DERs. A value of the order of one or a few seconds is reasonable. A further improvement of the distributed algorithm can be introduced to prevent the untimely activation of the algorithm. In detail, a delay time can be introduced so that each DER waits for a fixed number of steps in which saturation persists before sending the non-null error to the other DERs.

Table 1. Case 1 - Difference between optimal set points and nodal voltages, and norm of $\Delta \boldsymbol{V}^{sp}$ before and after the algorithm action.

Algorit.	$\boldsymbol{V}^{sp,opt} - \boldsymbol{V}$ (10^{-3}p.u.)						$\lvert\Delta V^{sp}\rvert_2$ (10^{-3}p.u.)
	DER_1	DER_2	DER_3	DER_4	DER_5	DER_6	
before	0.00	-3.47	0.00	0.00	0.00	0.00	3.47
after	0.96	-3.01	0.96	0.36	0.36	0.36	3.36

3. CASE STUDIES

The MV distribution test system depicted in Fig. 1 is built by duplicating the IEEE 13-bus Test Feeder, IEEE DSA Subcommittee (1992), after balancing its lines and loads. Accordingly, the power of the HV/MV transformer is doubled and assumed to be equal to 10 MVA. Three DERs are connected at each feeder, as shown in Fig. 1. Each DER can inject up to 600 kW and vary its reactive power injection between about ±300 kVAr (the exact value depending on the operating conditions of the network node and of the filter at the PCC).

The PSCAD 4.5 and MATLAB® R2010b environments have been adopted for the simulations. Two different load scenarios are considered: the full network load (equal to about 3 MW of active loads and 2 MVAr of reactive one) and half network load.

The local PI regulators have been designed according to Fusco and Russo (2024). Concerning the cooperative algorithm, the following matrix $\mathbf{L}$ have been derived,

$$\mathbf{L} = \begin{bmatrix} 0.6407 & -0.2306 & -0.2847 & -0.0834 & -0.0778 & -0.0720 \\ -0.1704 & 0.7239 & -0.1757 & -0.0834 & -0.0778 & -0.0720 \\ -0.2761 & -0.2306 & 0.6608 & -0.0834 & -0.0778 & -0.0720 \\ -0.0647 & -0.0876 & -0.0668 & 0.7349 & -0.2048 & -0.2287 \\ -0.0647 & -0.0876 & -0.0668 & -0.2196 & 0.6431 & -0.1895 \\ -0.0647 & -0.0876 & -0.0668 & -0.2651 & -0.2048 & 0.6342 \end{bmatrix} \tag{17}$$

Analyzing the elements of $\mathbf{L}$ it is evident that the algorithm assumes a stricter interaction among the group of DERs connected to the same feeder, see Fig. 1. It is due to the characteristics of the sensitivity matrix $\boldsymbol{\Gamma}$, because the voltage profiles of the two feeders are coupled only through the impedance of the substation transformer.

3.1 Case 1 – Load disconnection on the first feeder

It is assumed: full network load, all DER active power injections equal to 600 kW, and slack bus voltage equal to 1.05 pu. Starting from steady-state operating conditions, at time $t = 15\ s$ the load at bus 9 of the first feeder (0.843 MW–0.463 MVAr) is disconnected. The time evolution of voltages for the DERs of the first feeder is reported in Fig. 2. Each DER starts from a voltage equal to the optimal set point. When the loads are disconnected at t=15, voltage transients appear due to the action of the PI regulators, but DER_2 reaches saturation, so it is unable to reach the optimal set point, see Fig. 2.

After a time delay of 2 s (t=17 s), the cooperative algorithm intervenes with a time step equal to 1 s, and

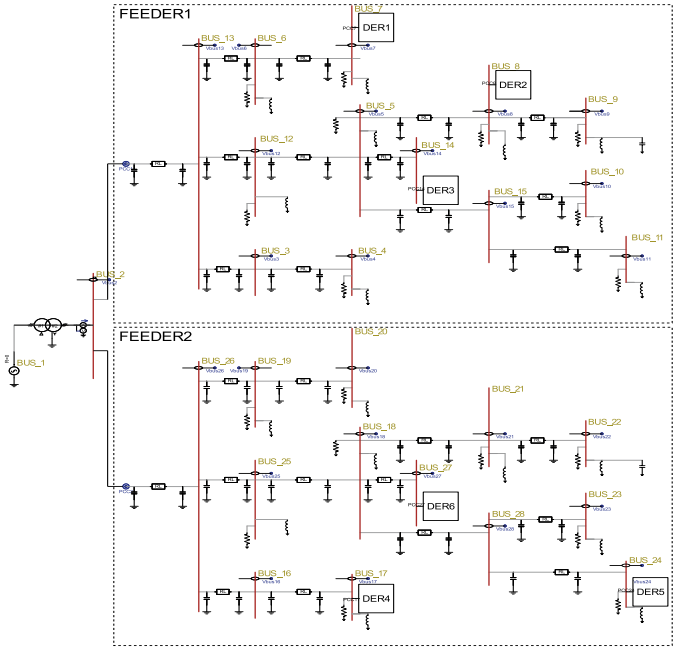

Fig. 1. PSCAD drawing of the two IEEE test feeders.

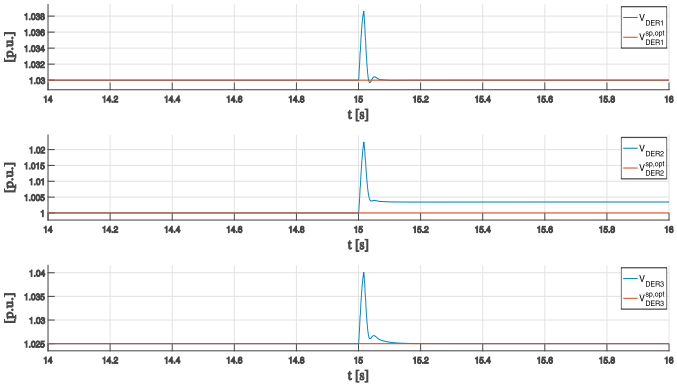

Fig. 2. Case1 - Trends of voltages and set points (before algorithm).

the other DERs help DER_2 to exit from saturation. The values of the difference between the optimal set points and the actual steady-state voltages are reported in Tab. 1; in particular, the first row refers to the values reached before the algorithm intervention, and the second row to the values reached after the algorithm convergence. Comparing the two rows, it is evident that

- before the algorithm intervention DER_2 is the only DER presenting a non-null difference due to saturation;
- the algorithm introduces a non-null value of the difference for all the DERs;
- the major contributions come from DER_1 and DER_3 that are connected to the same feeder as DER_2 (see also (17));
- the value of the difference for DER_2 is reduced by the algorithm.

The last column in Tab. 1 compares the values of $|\Delta V^{sp}|_2$ before and after the algorithm action, showing that the contribution of the other DERs reduces the distance of the voltage profile from the optimal set points. Figure 3 reports the time evolution of voltages and set points,

Table 2. Case 2 - Difference between optimal set points and nodal voltages, and norm of $\Delta \boldsymbol{V}^{sp}$ before and after the algorithm action.

Algorit.	$\boldsymbol{V}^{sp,opt} - \boldsymbol{V}$ (10^{-3}p.u.)						$\lvert\Delta V^{sp}\rvert_2$ (10^{-3}p.u.)
	DER_1	DER_2	DER_3	DER_4	DER_5	DER_6	
before	0.00	0.00	0.00	0.00	9.35	0.00	9.35
after	-0.92	-0.92	-0.92	-2.42	7.60	-2.42	8.49

showing the convergence of the distributed algorithm in 3 steps. The time evolution of reactive powers injected by the three DERs of the first feeder is reported in Fig. 4, evidencing the contribution of DER_1 and DER_3.

3.2 Case 2 – Load connection on the second feeder

It is assumed: half network load, all DER active power injections equal to 300 kW, and slack bus voltage equal to 1.03 pu. Starting from steady-state operating conditions, at time $t = 15$ s, a load (0.5 MW–0.5 MVAr) is connected to bus 23 of the second feeder. Similarly to the previous Case 1, the results in terms of the difference and the distance between the optimal and the actual voltage profiles are reported in Tab. 2. The time evolution of voltages and set points for the DERs connected to the second feeder are depicted in Fig. 5 and Fig. 6, respectively, before and after the algorithm intervention at time $t = 17$ s, whereas the time evolution of the reactive powers injected by the three DERs of the second feeder is reported in Fig. 7. From the first row of Tab. 2 and from Fig. 5, it is apparent that, after the load connection, DER_5 suffers reactive power saturation, and its voltage cannot reach the optimal set point.

After a time delay of 2 s (t=17 s), the cooperative algorithm intervenes, and the other DERs help DER_5 to exit from saturation. Comparing the two rows in Tab. 2, similar considerations can be made as the ones reported for the previous Case 1. In this case, the major contribution comes from DER_4 and DER_6 that are connected to the same second feeder as DER_5 (see also (17)). The last column of Tab. 2 evidences that the algorithm action reduces the distance of the actual voltage profile from the optimal one. Finally, from Figure 6 it is apparent that the distributed algorithm converges in 3 steps.

4. CONCLUSION

A distributed algorithm for the cooperation among DERs in the presence of reactive power saturation has been proposed. It determines the variation of the optimal voltage set points of the controllers of all the DERs using the voltage regulation errors and fixed averaging weights obtained from the ADN sensitivity matrix. The result is twofold: avoiding the persistence of voltage regulation errors caused by the wind-up phenomenon and getting a voltage profile closer to the optimal one. The communication requirements are quite limited. The distributed algorithm has been applied in numerical simulations, and the presented results validate the effectiveness of the proposed cooperative approach. In the considered MV test system, the distance from the optimal voltage profile is reduced of about $3 \div 9$ % thanks to the proposed algorithm. Future research will investigate the possibility of further improving these results.

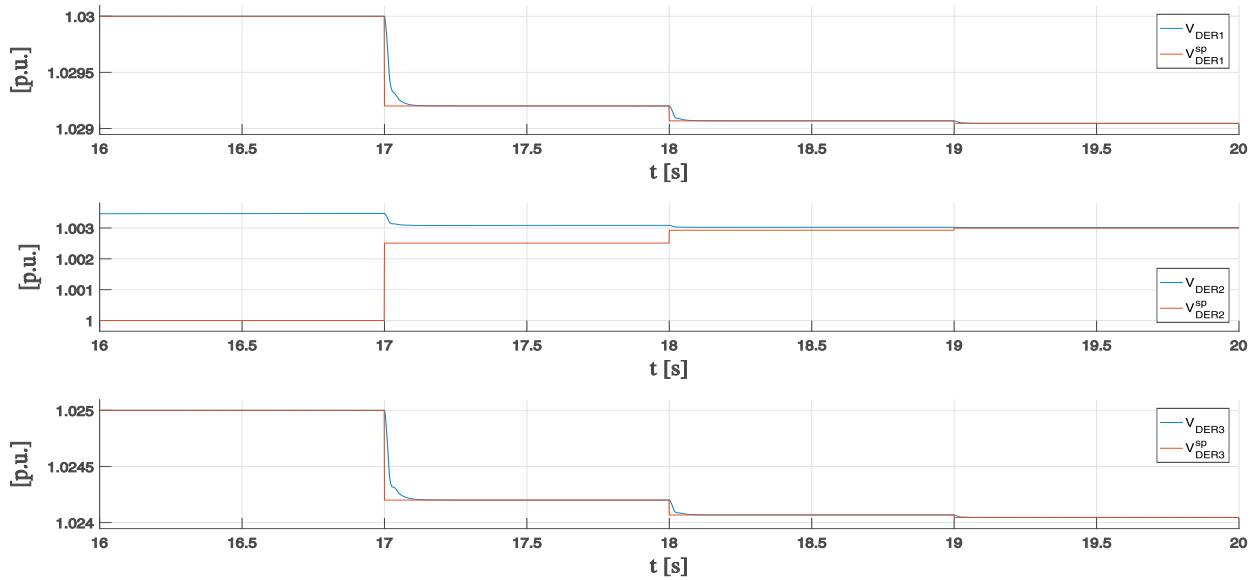

Fig. 3. Case1 - Trends of voltages and set points (after algorithm).

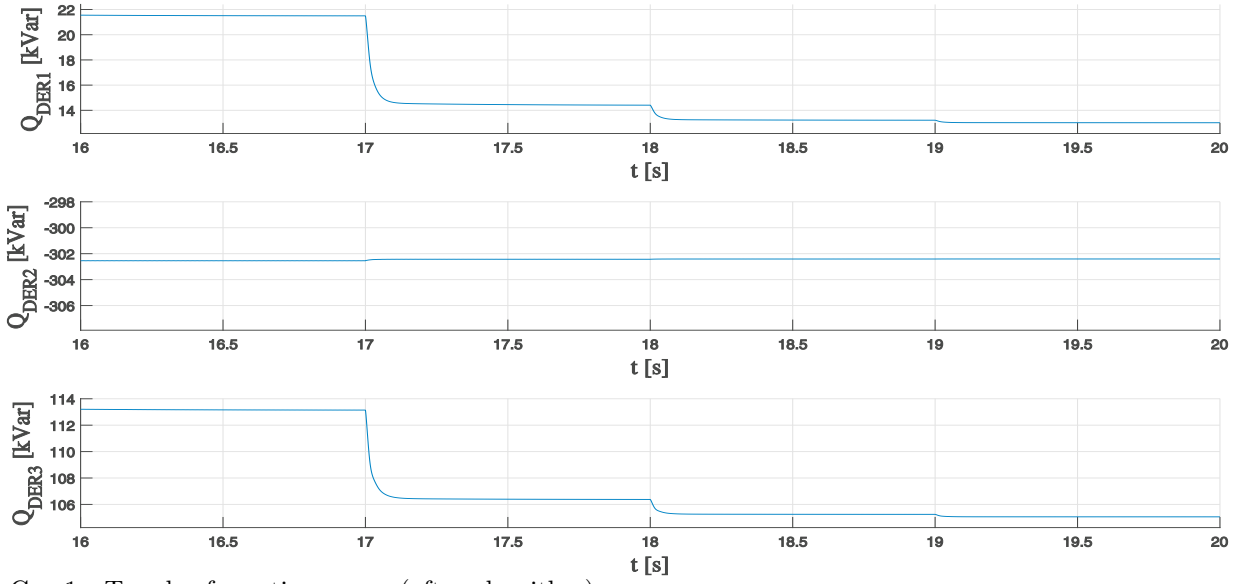

Fig. 4. Case1 - Trends of reactive power (after algorithm).

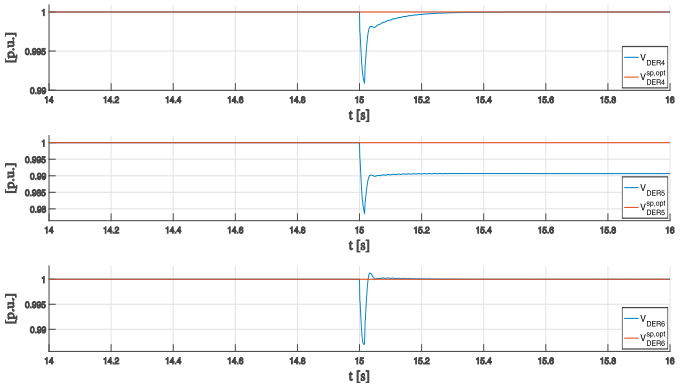

Fig. 5. Case2 - Trends of voltages and set points (before algorithm).

REFERENCES

Baran, M.E. and Wu, F.F. (1989). Optimal capacitor placement on radial distribution systems. *IEEE Transactions on Power Delivery*, 4(1), 725–734.

Bidram, A., Lewis, F.L., and Davoudi, A. (2014). Distributed control systems for small-scale power networks: Using multiagent cooperative control theory. *IEEE Control systems magazine*, 34(6), 56–77.

Edwards, C. and Postlethwaite, I. (1997). Anti-windup schemes with closed-loop stability considerations. In *1997 European Control Conference (ECC)*, 2658–2663. IEEE.

EN 50549 (2019). Requirements for generating plants to be connected in parallel with distribution networks. European Standard, CENELEC, Brussels.

Errouissi, R. and Al-Durra, A. (2018). A novel control technique for grid-tied inverters considering unbalanced grid voltage conditions and control input saturation. *IEEE Transactions on Sustainable Energy*, 10(4), 2223–2234.

Fusco, G. and Russo, M. (2024). Local der control with reduced loop interactions in active distribution networks. *Energies*, 17(9). doi:10.3390/en17091991. URL `https://www.mdpi.com/1996-1073/17/9/1991`.

Fusco, G., Russo, M., and Casolino, G.M. (2023). Voltage and active power local pi control of dis-

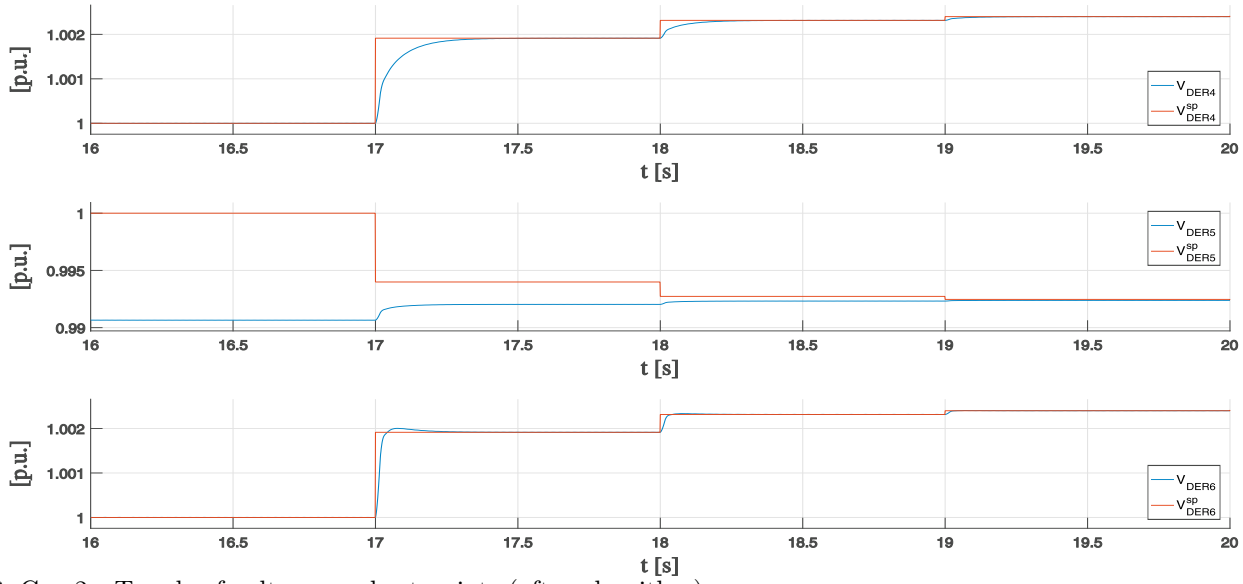

Fig. 6. Case2 - Trends of voltages and set points (after algorithm).

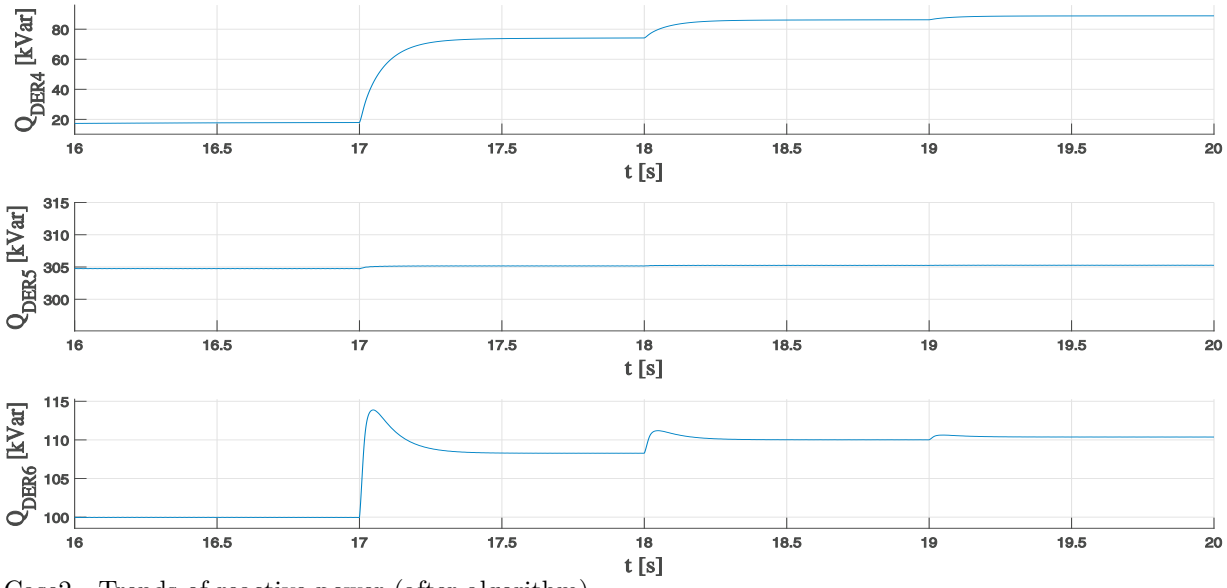

Fig. 7. Case2 - Trends of reactive power (after algorithm).

tributed energy resources based on the effective transfer function method. *International Journal of Electrical Power & Energy Systems*, 152, 109264. doi: https://doi.org/10.1016/j.ijepes.2023.109264.

Fusco, G., Russo, M., and De Santis, M. (2021). Decentralized voltage control in active distribution systems: Features and open issues. *Energies*, 14(9). doi:10.3390/en14092563. URL `https://www.mdpi.com/1996-1073/14/9/2563`.

IEEE DSA Subcommittee (1992). IEEE PES Test Feeder. URL `https://cmte.ieee.org/pes-testfeeders/`. accessed on February 2025.

IEEE Std 1547™-2018 (2024). IEEE application guide for IEEE Std 1547™-2018, IEEE standard for interconnection and interoperability of distributed energy resources with associated electric power systems interfaces. Guide, IEEE. doi:10.1109/IEEESTD.2024.10534228.

Lin, Z. (2019). Control design in the presence of actuator saturation: from individual systems to multi-agent systems. *Science China. Information Sciences*, 62(2), 26201.

Morilla, F., Garrido, J., and Vázquez, F. (2009). Anti-windup coordination strategy for multivariable pid control. In *2009 IEEE Conference on Emerging Technologies & Factory Automation*, 1–7. IEEE.

Mulder, E.F., Kothare, M.V., and Morari, M. (2001). Multivariable anti-windup controller synthesis using linear matrix inequalities. *Automatica*, 37(9), 1407–1416.

Robbins, B.A., Hadjicostis, C.N., and Domínguez-García, A.D. (2013). A two-stage distributed architecture for voltage control in power distribution systems. *IEEE Transactions on Power Systems*, 28(2), 1470–1482. doi: 10.1109/TPWRS.2012.2211385.

Zhu, H. and Liu, H.J. (2016). Fast local voltage control under limited reactive power: Optimality and stability analysis. *IEEE Transactions on Power Systems*, 31(5), 3794–3803. doi:10.1109/TPWRS.2015.2504419.

Zhuang, K., Xin, H., Hu, P., and Wang, Z. (2022). Current saturation analysis and anti-windup control design of grid-forming voltage source converter. *IEEE Transactions on Energy Conversion*, 37(4), 2790–2802.